MODULATION OF MEG SIGNALS DURING OVERT AND IMAGINED WRIST MOVEMENT FOR BRAIN-COMPUTER INTERFACES

by

Gustavo Pittella Sudre

B.S. in Computer Science, University of Kansas, 2006

Submitted to the Graduate Faculty of

Swanson School of Engineering in partial fulfillment

of the requirements for the degree of

Master of Science

University of Pittsburgh

2008

UNIVERSITY OF PITTSBURGH

SWANSON SCHOOL OF ENGINEERING

This thesis was presented

by

Gustavo Sudre

It was defended on

November 21st, 2008

and approved by

Wei Wang, PhD, Assistant Professor, Department of Physical Medicine and Rehabilitation

Aaron Batista, PhD, Assistant Professor, Department of Bioengineering

Anto Bagic, PhD, MD, MSc, Assistant Professor, Neurology and Neurological Surgery

Thesis Advisor: Doug Weber, PhD, Assistant Professor, Department of Physical Medicine and Rehabilitation

MODULATION OF MEG SIGNALS DURING OVERT AND IMAGINED WRIST MOVEMENT FOR BRAIN-COMPUTER INTERFACES

Gustavo Sudre, M.S.

University of Pittsburgh, 2008

This work uses Magnetoencephalography (MEG) to investigate movement-related neural activity in the cerebral cortex. MEG is an effective non-invasive tool to study cortical activity because it has higher temporal and spatial resolutions than other non-invasive methods, such as fMRI and EEG. One objective of the proposed study is to characterize MEG signal modulation during overt and imagined movements. Such characterization can then be implemented to study motor control and cortical plasticity. In the future, this information can be used to aid the mapping of motor regions of the brain prior to surgical implantation of electrodes for brain-computer interface (BCI) applications. For the current experiments, four right-handed subjects were asked to perform wrist movements with their dominant hand in four directions (radial deviation, ulnar deviation, flexion, and extension) following a visual cue (up, down, left, and right, respectively). In separate sessions, subjects were then asked to imagine performing the same movements following the visual cue. Frequency-domain analysis of the MEG signals reveals consistent modulation during both overt and imagined movements on sensors overlaying sensorimotor areas of the brain. Modulation preceded movement onset and was characterized as a decrease in power in low frequency bands (10-30Hz) and increase for lower bands (0-10Hz), starting 200 ms after the visual cue and lasting 500 ms, which was accompanied by an increase of power in the 65-90Hz band during the same period. This sequence is followed by an increase in power in the 10-30Hz band. Several of these modulations in cortical activity were also

significantly tuned ($p < 0.05$) to movement direction in both overt and imaginary tasks. Two methods were used for decoding: Optimal Linear Estimator (OLE) and Bayesian. The decoding accuracy of a given target for the imagined wrist movement data varied among subjects from 29.4% to 49.75% (mean: 41.4%) correct trials for OLE, and 30.1% to 50.9% (mean: 41.5%) for Bayesian. For overt wrist movement data, decoding accuracy for a given target ranged from 34.1% to 67.4% (mean: 48.3%) correct trials for OLE, and 33.1% to 66.9% (mean: 48.0%) for Bayesian. MEG can detect cortical areas that show significant modulation during overt and imagined wrist movement. We conclude that MEG can be an important tool for quantitatively studying cortical activity for motor tasks, conducting non-invasive BCI research in humans, and pre-surgical identification of optimal implantation sites of microelectrodes for neuroprosthetic control.

TABLE OF CONTENTS

LIST OF TABLES

LIST OF FIGURES

PREFACE

I would like to greatly thank Doug Weber for his mentorship and advising throughout my work, and Wei Wang for his help and guidance for the majority of this project. I would also like to acknowledge all my lab mates that gave me important insights through this journey. Finally, I'd like to dedicate this work to my family, that gave me the means and encouragement to be here, and to Kim, because without her support and understanding none of this work could have been accomplished.

1.0 INTRODUCTION

Magnetoencephalography (MEG) is an efficient non-invasive tool to study cortical activity because of its high temporal and spatial resolutions. The main goal of this project is to use MEG to investigate movement-related neural activity in the cerebral cortex. Such knowledge can then be used for studying human motor control and non-invasive brain-computer interfaces research, as well as for localizing optimal implantation sites of microelectrodes for neuroprosthetic applications.

1.1 BACKGROUND

Brain-machine interfaces (BMIs) have the potential to provide people with severe motor impairments the ability to control devices that act in their environment, such as computers, power wheelchairs, and prosthetics. This technology has been studied for a few decades using different methods for neural recording and signal processing (Schwartz, et al. 2006). One of the key factors for a successful BCI application is identifying cortical representation of movement, and several studies have previously shown that hand movement (e.g. hand positions, movement direction and speed) can be predicted from the activity of populations of motor cortical neurons (Georgopoulos, Schwartz and Kettner 1986) (Moran and Schwartz 1999) (Wang, et al. 2007). The work presented in this thesis focuses on studying how MEG can be used to study the cortical

representation of movement, and also to better examine cortical processes that can be used to control BMIs. As a research tool, MEG can be used to locate optimal sites in the brain for implantation of electrodes, as well as to conduct pre-surgical training of subjects so they learn to better modulate brain activities in order to control BMIs.

MEG has been previously used in a wide variety of studies, from sensory mapping (Druschky, et al. 2003), to attention (Amorim, et al. 2000), language (Kim and Chung 2008), and neurological disorders (Georgopoulos, et al. 2007), because of its superior temporal (less than 1 millisecond) and spatial (several millimeters) resolutions (Hari and Forss 1999). It records the magnetic activity generated by the electrical currents, which can be modeled as dipoles, produced by neuronal activity in the brain. It is estimated that about 10^4 to 10^5 neurons must be simultaneously activated to generate a signal strong enough to be captured by MEG sensors. These sensors are usually magnetometers (measuring the absolute magnitude of a magnetic field) or gradiometers (measuring the gradient of the magnetic field), which can be planar or radial depending on the position of the sensing coils (Diekmann and Becker 1999). The magnetic activity captured by MEG is generated by the post-synaptic activity of neurons, which is slow enough (compared to action potentials) to allow for temporal summation.

The dipole sources of magnetic activity detectable by MEG are thought to be tangential to the skull (see Figure 1). Conversely, MEG has difficulties capturing dipole sources radial to the skull (Hämäläinen, et al. 1993). This property of MEG contrasts with the characteristics of electroencephalography (EEG), arguably the most commonly used recording technique in BCI applications to date, which has its strengths in capturing sources located radially to the skull. Therefore, EEG and MEG can be used complementarily. Another important point to mention is

that while some of the electric activity in the brain gets attenuated and spatially smeared by the skull, the magnetic fields pass through it undistorted.

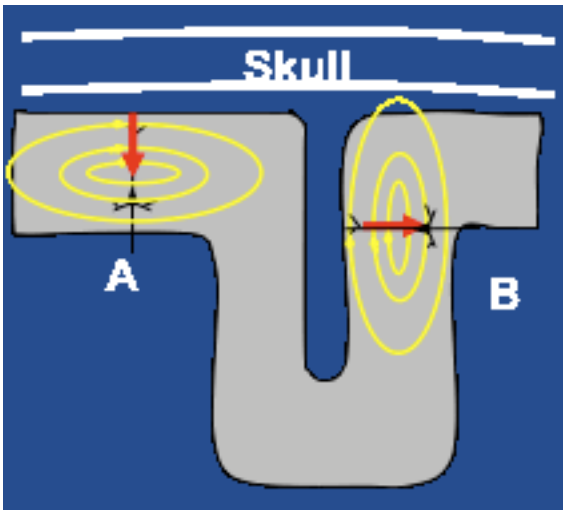

Figure 1: A schematic drawing illustrating neuronal activity captured by MEG. The figure depicts a layer of cortical tissue and one of its folds. MEG can record magnetic activity generated by Neuron B, but not Neuron A. The red arrows show the direction of the dendritic current and the equivalent dipole, and the yellow curves represent the magnetic fields induced by the dendritic activity.

Previous studies have also analyzed MEG activity for BCI purposes during motor tasks, but this is the first work to focus decoding the target choice for both overt and imagined wrist movements. Waldert et al. used EEG and MEG signals to decode target choice based on subject-chosen movements of a joystick to 4 different targets (Waldert, et al. 2008). They found increase in the power of bands lower than 7 Hz (low-frequency band) and 62– 87 Hz (high-γ band) and a decrease for 10 –30 Hz (β band), but only found useful decoding information in the low-frequency bands. Georgopolous et al. had subjects draw a pentagon with a MEG-compatible joystick (also without visual feedback), and during offline analysis the researchers were able to reconstruct with acceptable accuracy the 2D trajectory using a linear summation of weighted

contributions of the MEG signals (Georgopoulos, et al. 2005). Finally, Mellinger et al. trained in about half-hour a group of subjects to modulate their sensorimotor μ and β rhythms (10-12Hz and 20-24Hz, respectively) to control a MEG-BCI in real-time (Mellinger, et al. 2007). They used imagined limb movements to send binary decisions to control the feedback paradigm (upward or downward movement of the cursor).

Compared to previous works, this study aims to achieve a reasonable decoding accuracy using both overt and imagined wrist movements to four possible directions. By comparing different decoding algorithms, two viable options for target decoding are analyzed regarding accuracy and speed, which will be used in a real-time MEG-BCI in the near future. Also, Leuthardt et al. have shown with ECoG (Electrocorticography) that the high-frequency bands (60-200Hz) carry important information about the direction of movement (Leuthardt, et al. 2004), and high frequency bands have also been shown to be related to other brain functions, such as visual perception, attention, memory, and self-paced movements (Kaiser, et al. 2003) (Crone, et al. 2001) (Cheyne, et al. 2008). This study hopes to evoke a stronger high-frequency response by providing visual feedback of the cursor position to the subject, which will better engage his or her attention to the task. Finally, the magnetic activity in each sensor will be analyzed to characterize the evolution of the MEG signal over time across the whole head.

1.2 SPECIFIC AIMS

This work focuses on characterizing and comparing MEG activity during overt and imagined wrist movement in the temporal and frequency domains. It is hypothesized that evoked potentials (peaks) will show increasing latencies with respect to visual stimulus onset, as the signal travels

from visual to motor cortex. Also, it is expected that sensors closer to the sensorimotor area of the cortex will exhibit a decrease and a subsequent increase of the power of low frequency bands with respect to the baseline, accompanied by an increase in the activity of the high frequency bands.

Another goal of this study is to examine tuning to target direction for different frequency bands, and then decode movement direction for both overt and imagined conditions using two different algorithms: Optimal Linear Estimator (OLE) and Bayesian inference. This study will also investigate advantages and disadvantages of both methods for decoding movement direction from multi-channel MEG recording.

2.0 METHODS

This study is approved by the Institutional Review Board (IRB) at the University of Pittsburgh, and all experiments were in accordance with IRB protocol number 07110181. Four subjects were recruited. They were right-handed and their ages varied between 25 and 40 years old. Magnetic fields generated by brain activity were recorded while the subject performed a center-out task using the right wrist. MEG signals were digitized at 1Khz, high-pass filtered at 0.1Hz and low-pass filtered at 330Hz.

2.1 RECORDING METHODS

The MEG Vectorview system by Elekta Neuromag® (http://www.elekta.com/) was used to record brain activity. This system has a total of 306 channels, of which 102 are magnetometers and the other 204 are planar gradiometers. They are distributed in 102 sensor triplets, each of them containing one magnetometer and two gradiometers: one measuring the differential magnetic field in the longitudinal direction and the other in the latitudinal direction. Figure 2 shows the location of the 102 sensors triplets in the MEG helmet.

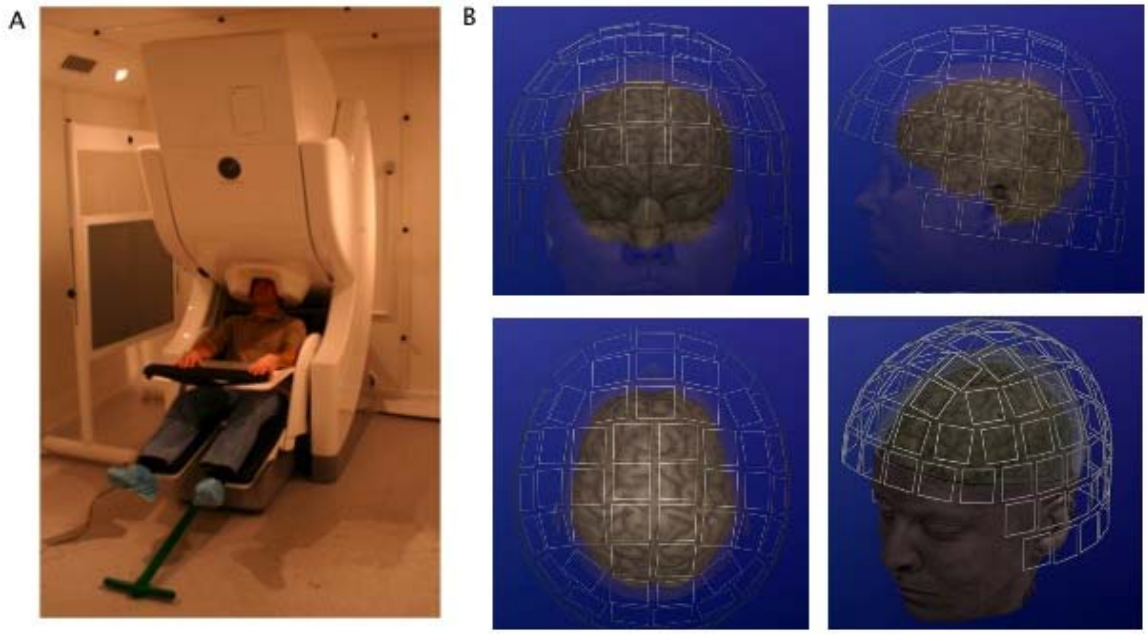

Figure 2: A. Subject sitting in the Elekta Neuromag® MEG machine. Projection screen was placed to the side to show the subject. **B:** Placement of the 102 sensors within the helmet (Neuromag, Elekta 2006). Each sensor has one magnetometer and two gradiometers.

Muscle activity (electromyography – EMG) of wrist flexor and extensor muscles (flexor carpi radialis and extensor carpi radialis) was recorded in all sessions. Electrooculography (EOG) was recorded with electrodes placed above, below, and lateral to the eyes. EOG captured horizontal and vertical eyes movements, as well as eye blinks. Additionally, four head position indicator (HPI) coils were placed on the subject's scalp to record the position of the head with relation to the MEG helmet at the beginning of each session. These coils, along with three cardinal points (nasal, left and right pre-auricular), were digitized into the system and were later used for pre-processing of the data for head movement compensation.

2.2 EXPERIMENTAL SETUP

Subjects were asked to perform wrist movements with their right (dominant) hand in four directions (radial deviation, ulnar deviation, flexion and extension) following a visual cue (up, down, left, and right, respectively) while holding a MEG-compatible joystick (Current Designs Inc. - http://www.curdes.com). They were instructed to make movements solely with their wrist, keeping shoulder and arm at rest. The wrist was chosen not only because of previous studies relating cortical tuned activity to wrist movement (Kakei, Hoffman and Strick 1999), but also because it is relatively far from the MEG helmet, therefore reducing EMG contamination of the signal. Monitoring EMG of wrist flexor and extensor muscles was also important to make sure that subjects were not moving or co-contracting muscles during imagined sessions. BCI2000, a general purpose brain-computer interface software (Schalk, McFarland and Hinterberger 2004), was used to present the stimulus and to track joystick position. The joystick was adapted to be controlled with wrist movements only (Figure 3).

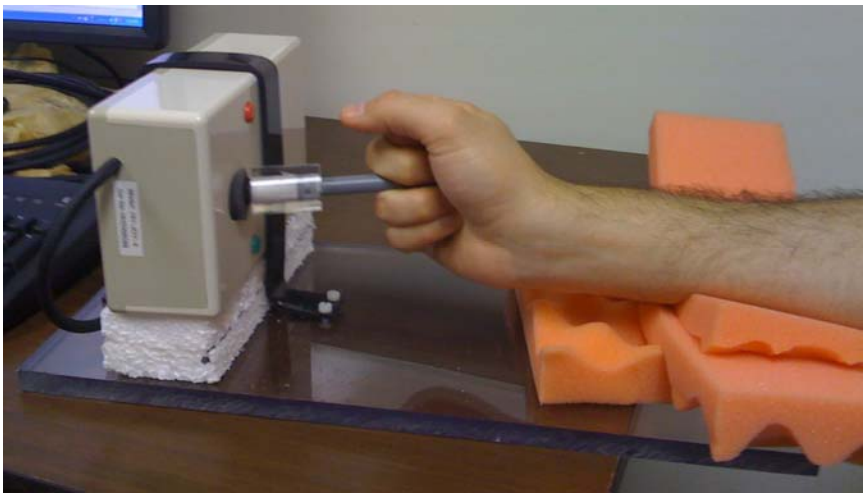

Figure 3: MEG-compatible joystick modified to capture wrist movements. The joystick handle was made of plastic in the shape of a T where the subject would grasp to control the joystick. Foam cushion was used to stabilize the arm and allow the subject to perform the movements solely with the wrist.

The subject had visual feedback of the cursor position during the whole session, and each session was divided into equal number of random repetitions per target. A repetition starts after the subject holds the cursor in the center target, which triggers the appearance of one of the four peripheral targets. In a successful repetition, the subject needs to move the cursor to the target while fixating the eyes in the center of the screen, and then hold the cursor position at the target. If the subject overshoots for the target, or does not get there within a pre-determined amount of time, the trial is aborted. The timing information for the repetitions can be seen in Figure 4.

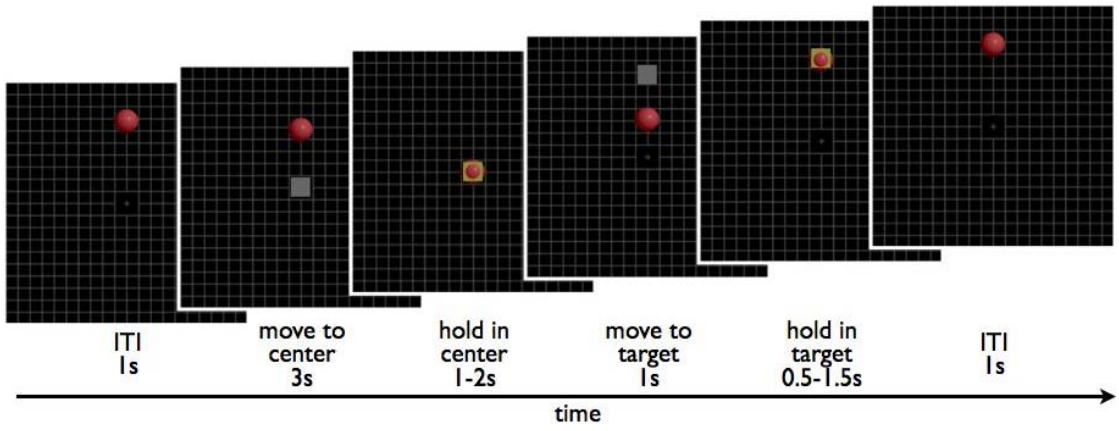

Figure 4: Visual feedback of the center-out task. The cursor needs to go to the center and stay there for a hold period until the peripheral target appears. Then the cursor moves to the target and stays there until the successful repetition is finished. The target changes color when it is hit by the cursor, and disappears when the holding period has finished. The time spent in each session is depicted in the picture. (ITI: inter-trial interval).

In separate sessions, the same subjects were then asked to imagine performing the same wrist movements following the visual cue. The cursor moved with a fixed speed toward the target after a random delay of 0.5-1 seconds, which simulated the time the subject had to react to the target appearance. In order to keep the subject engaged in the task, catch trials were inserted. During a catch trial, the cursor stopped moving before it reached the target. The subject was instructed to press one of the joystick buttons when a catch trial was recognized.

Overt and imagined tasks were recorded in different sessions. Regardless of the type of the session, the subject was instructed to always hold the joystick handle with the right hand and position the left hand ready to press the joystick button. For both types of sessions, in order to minimize eye movements the subjects were asked to fixate their eyes in a cross-hair in the center of the screen throughout the whole repetition (starting when the target appears at the center). It was acceptable to relax the eyes and blink during the inter-trial interval (ITI) after one of the

peripheral targets disappeared. Also, the projection screen was positioned at a distance from the subject to minimize saccades to the targets.

Finally, before any overt or imagined tasks were recorded for a given subject, data was acquired to quantify the amplitude of his/her characteristic eye-movement. The four targets were displayed separately in the screen while the cursor moved linearly to them (similarly to the imagined task) for 3 repetitions per target. The subject was asked to move the eyes in the direction of the target when it came up in the screen.

2.3 DATA ANALYSIS

2.3.1 Pre-processing

The first step in the analysis process was to perform a spatial filtering on the data using the Signal Space Separation (SSS) (Taulu, Simola and Kajola 2005) method. SSS will first compensate head movement between sessions and realign all sessions' data so that they correspond to the same head position. SSS will then spatially filter the data so that only signals coming from sources within a sphere inside the MEG helmet will be kept, and signals coming from sources outside the MEG helmet will be suppressed, which is shown in Figure 5. SSS also minimizes the effects of sensor noise. In the current setup at the MEG center, head position can only be recorded at the beginning of each session (each session is approximately 5 to 6 minutes with 20 movements to each target). It is assumed that the subject's head position remained constant throughout the session.

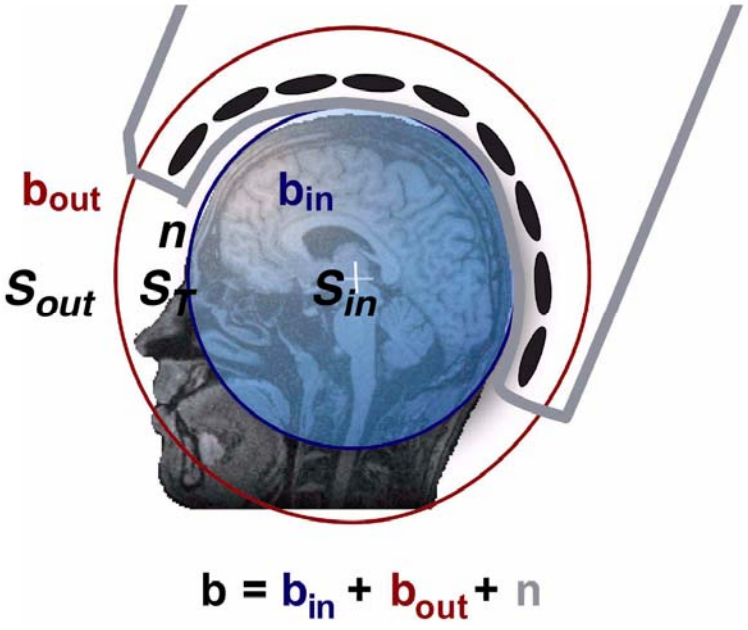

Figure 5: Schematic illustration of how the SSS algorithm works (Neuromag 2006). By using the position of the HPI coils and fiducial points, SSS projects a sphere to represent the brain inside the sensor array (space $\mathbf{S_{in}}$). Noise **n** coming from space $\mathbf{S_T}$ represents artifacts generated by sources close to the helmet and the sensors themselves. $\mathbf{B_{out}}$ is the magnetic field coming from $\mathbf{S_{out}}$, representing all external sources to the helmet.

Stimuli presentation was synchronized with the MEG recording system through parallel port impulses sent from the computer generating the stimuli. The MEG recording machine saved these impulses which were then used to crop the data into individual repetitions. Data for each repetition spans 1s before the peripheral target appeared and 1.5s after. Additional information about the outcome of the repetition (if the subject successfully hit the target) was also extracted from these impulses.

The last step was to discard repetitions contaminated by eye movements, because such activity may bias the data towards certain targets. The threshold of 150mV was applied to each

repetition and whenever the peak-to-peak amplitude of the signal of either EOG channel (i.e. horizontal or vertical) crossed this threshold, the repetition was marked as invalid. The EOG data containing subject-specific intended eye movement cued by the appearance of peripheral targets were also analyzed, and in for all subjects the peak-to-peak amplitude was higher than the 150mV used as threshold.

Wrist movement onset was determined by differentiating the cursor position with respect to time and identifying the instant when the velocity trace reached 10% of its peak. Conversely, movement offset was taken as the last time when a value bigger than 10% of the velocity peak was observed. Only repetitions that did not show eye movement contamination and hit the target were used in the analysis. Each repetition had its own baseline, taken as the 1s before target onset.

2.3.2 Time-domain analysis

MEG signals were aligned based on target onset, averaged across repetitions for each target, low-pass filtered at 10Hz (6^{th} order Butterworth IIR filter) and detrended. The peak onset for each channel was taken as the first moment after target onset when the averaged trace crossed ±2 standard deviations from the baseline.

2.3.3 Frequency-domain analysis

The data first were notch-filtered at 60Hz, 120Hz, and 180Hz (Butterworth 4^{th} order) to remove line noise and its harmonics, and then converted to the frequency domain using the Maximum

Entropy Method (MEM) (McFarland, Lefkowicz and Wolpaw 1997). Baseline period is defined as the 1 second prior to visual cue onset.

For time-averaged analysis, MEM output (28^{th} order) consisted of a single value for each frequency from 0 to 200Hz (3Hz steps), corresponding to the power of that frequency during the baseline period. The power for the movement period was calculated similarly in the period from target onset to movement offset. For continuous time analysis, the spectrograms were generated by using a sliding window from -1 to 1.5 sec (200ms window with 50ms steps). Change from baseline is calculated as defined in (1).

$$Chg = \frac{power - baseline}{baseline} \times 100 \quad (1)$$

2.3.4 Decoding

Two different algorithms were used for decoding: Optimal Linear Estimator (OLE) and Bayesian inference. The different frequencies were divided into the following bands: 0 – 4Hz, 4 – 12Hz, 12 – 30Hz, 30 – 55Hz, 65 – 90Hz, 90 – 115Hz, 125 – 150Hz, 150 – 175Hz, 185 – 200Hz. The power change from baseline was averaged across the frequencies in the band. The (channel - frequency band) pair was called a feature. Given 306 MEG channels and 9 frequency bands per channel, there are 306 * 9 = 2754 features. For decoding purposes only, the features contained the log of the change, and not the change itself.

Feature selection was done by using a one-way ANOVA, which was applied to individual feature by comparing power of each feature across four different targets. This way, each feature had a p-value associated with it that meant the probability of the data for all four targets had

come from the same distribution. In other words, the smaller the p-values, the more different the data of that feature was per target position.

Finally, movement direction was decoded from MEG signals both with single-trial data and with data averaged over multiple trials or repetitions. For single-trial decoding, the leave-one-out method was used such that the decoding algorithms were trained with all the data set except for one repetition, which was then used for decoding. This was done for all the repetitions recorded for the subject, and the accuracy for a given target was measured as in (2), where *reps* represented the total number of repetitions for the given target and *errors* represent how many repetitions were incorrectly decoded.

$$\frac{reps - errors}{reps} \times 100 \qquad (2)$$

Averaged data decoding was done by averaging a given number of repetitions for movement toward the same target before using them as the testing set for decoding. These repetitions were chosen randomly without replacement from the repetition pool and the rest of the data were used for training. This process was repeated always 100 times (*reps* = 100 in (2))). This study examined decoding accuracies using data averaged over 2, 4, 6, 8, 10, 15, and 20 repetitions.

2.3.4.1 Optimal Linear Estimator

The OLE method (Salinas and Abbott, 1994) was implemented as the matrix operation shown in (1), where *K* contained the kinematic predictions for each repetition and *P* the power change value for each feature being used.

$$K_{2Xreps} = W_{2Xfeat} \times P_{featXreps} \qquad (1)$$

The weight matrix W was calculated during training using the pseudo-inverse matrix of P as shown in (2).

$$W_{2Xfeat} = K_{2Xreps} \times (P_{featXreps})^{-1} \quad (2)$$

It is important to note that the rows of K represented the Cartesian coordinates of each target (e.g. right was [1 0], down was [0 -1]).

2.3.4.2 Bayesian

Bayesian decoding was performed using Bayes' theorem shown in (3), where the left term represented the probability of one of the four targets given a certain change in power. Two important points needed to be considered when using a Bayesian approach: how to obtain the probability of a given change in power and how to combine the probability results of different features.

$$P(tgt \mid pwr) = \frac{P(tgt) \times P(pwr \mid tgt)}{P(pwr)} \quad (3)$$

Because of the number of samples recorded for each target, the log transformation performed in the data, and most importantly the Central Limit Theorem, it was assumed that each probability came from a normal distribution. For computational purposes, these distributions were obtained by simulating a Normal distribution with mean and variance obtained from the data for each feature. Finally, the probabilities for each feature were combined in a final probability for a target by multiplying all the individual probabilities.

3.0 RESULTS

3.1 TIME-DOMAIN ANALYSIS

The cortical activity recorded with the whole-head MEG system showed a clear temporal order of activation from visual to motor cortex for both overt and imagined movements in all subjects. Figure 6 shows the averaged time series for three MEG gradiometers on top of the occipital, parietal, and frontal lobes during visually-guided wrist movement. The peak latencies with respect to target onset for these three MEG channels are approximately 150ms, 200ms, and 300ms, respectively, suggesting a propagation of information from the visual to the motor cortices.

Another important point to consider is that movement usually occurred around 450ms, so all three evoked potentials precede the movement, and all of them go back to baseline values around 700ms. It is also interesting to notice that, for the sensor on top of the motor cortex, its peak amplitude is significantly lower for imagined than for overt movement, suggesting that this signal is more related to the motor output.

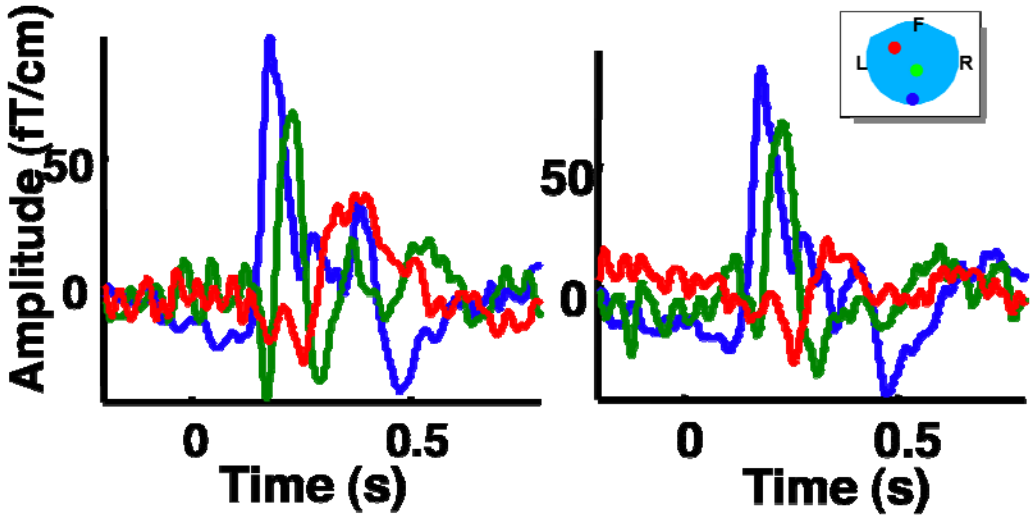

Figure 6: Details of the MEG traces for three different gradiometers in overt and imagined conditions (left and right, respectively). Inset shows the location of the channels in the helmet, where F denotes the front of the helmet, and L and R the left and right ears. The red channel is assumed to cover motor cortex, green is parietal, and blue is visual. The traces were low-pass filtered at 40Hz and represent an average of all the repetitions for subject S1 (approximately 100 repetitions) for a given target. Time 0 is target onset.

Figure 7 shows the temporal evolution of MEG signal amplitude over the whole head. It is evident that the contra-lateral sensorimotor areas were activated around 0.5 sec after target onset with a clear dipole pattern composed of a positive peak of 100fT/cm and a negative peak of 50fT/cm.

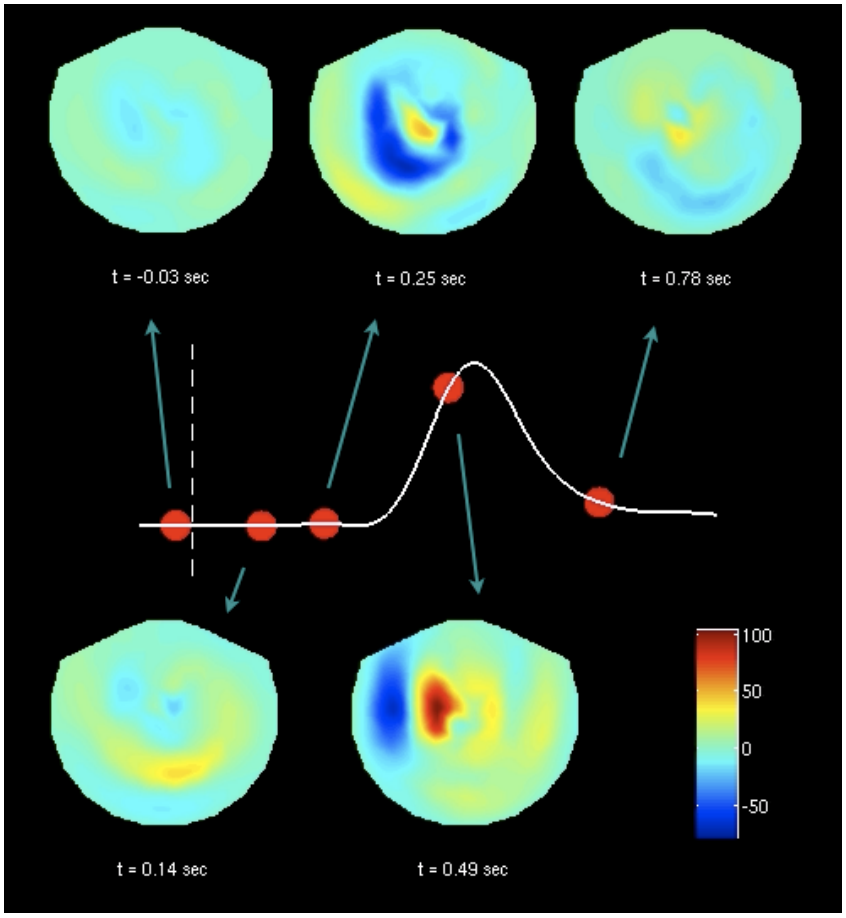

Figure 7: MEG signal amplitude over the whole head and across time for overt movements. This figure shows cortical activity at five different time points with five color plots/snapshots showing MEG signal amplitude across the head. MEG signals were averaged across all targets and repetitions for subject S3 and low-pass filtered at 40Hz. Color represents MEG signal amplitude with units of fT/cm. The white trace shows velocity profile, with target onset marked by the dotted line. Red circles on the velocity profile and arrows indicate the time points when the snapshots were taken.

3.2 FREQUENCY-DOMAIN ANALYSIS

The first step of the data analysis in the frequency domain was to examine which cortical areas showed clear modulation of frequency bands during movement. Figure 8 shows the spatial and temporal patterns of low frequency band (10-30Hz) modulation. During movement time there is a decrease in the power for the low frequency band, and after the movement there is a rebound or increase in power of the same band. Overall, the strongest low frequency band modulation occurs in the sensors around the sensorimotor area, and both the overt and imaged movements show a similar spatiotemporal pattern of modulation.

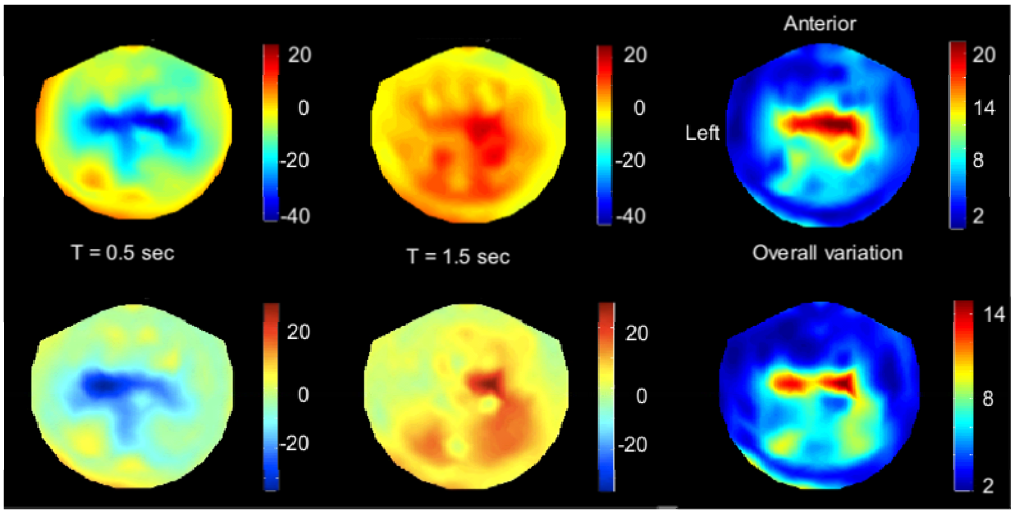

Figure 8: Modulation of mu and beta bands over time. Top row corresponds to overt movement and the bottom row corresponds to imagined movement. Right-most plots show the overall modulation during movement. Data were averaged over targets and repetitions. Time 0 (T=0) is target onset. Color bars for first two columns represent the percent of modulation from baseline, and color bar for last column shows the total percent modulation over the trial period.

Figure 9 shows the power spectrum for an MEG sensor during both overt and imagined movement as an example of the pattern of modulation encountered among subjects.

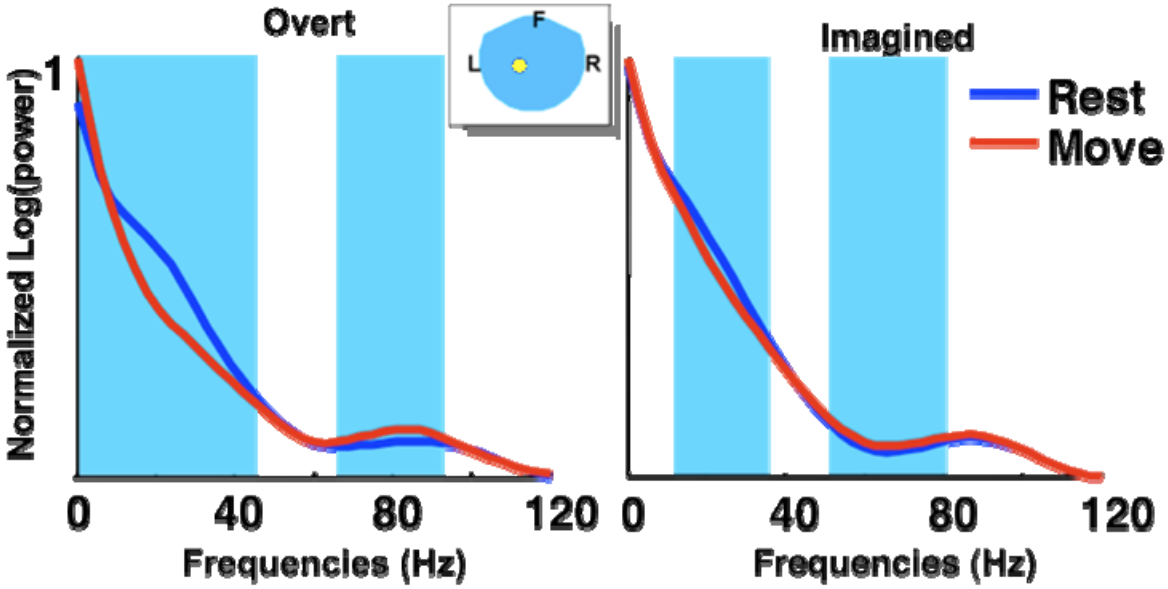

Figure 9: Comparison of frequency power for movement and rest during overt and imagined conditions for subject S3. Data for one gradiometer situated over the contralateral sensorimotor area (see inset), averaged over all targets (162 repetitions per target) during move and baseline periods (red and blue traces, respectively). Light blue shades show significant differences ($p < 0.05$).

The figure shows a decrease in power of low frequency bands as well as an increase in power for high bands in both overt and imagined conditions. More specifically, the overt condition causes significant decrease in activity of lower bands up until 40Hz, and also an increase of activity of bands from 65Hz to 90Hz. The power decrease of low frequency bands for imagined movement goes from 10-35Hz, and the increase happens in the range of 50-80Hz. Overall, the change from rest to move conditions is more evident in overt than imagined condition.

After showing that there is significant modulation of several frequency bands during the task, a closer look was necessary to understand how these modulations evolve over time. Figure 10 depicts this evolution for the same channel analyzed above.

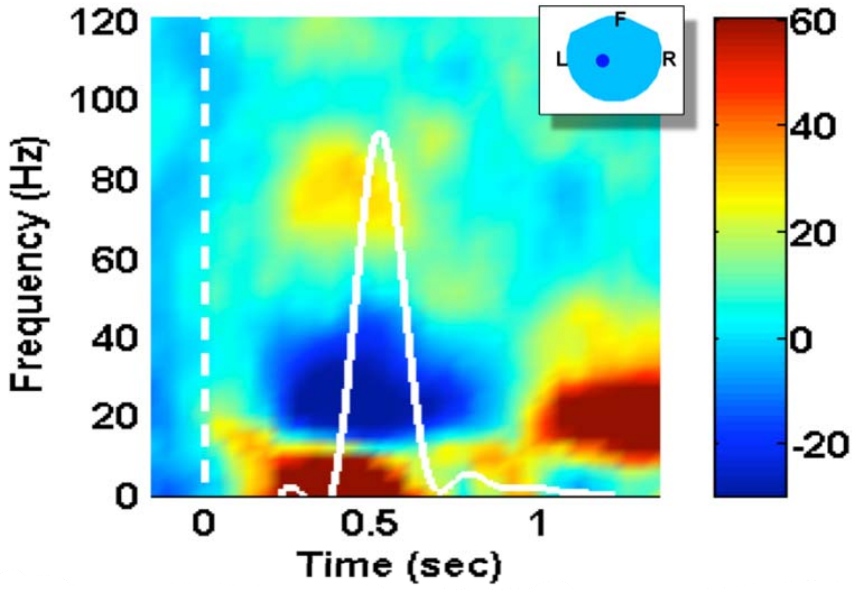

Figure 10: Frequency modulation evolution over time. Hotter colors indicate percent increase in power with respect to the baseline. White vertical dashed line shows the onset of the target and the solid white trace is the velocity profile of the cursor in the screen. Data from overt movement averaged over all targets and repetitions (162 repetitions per target) for subject S3, aligned on visual cue onset.

The power modulation over time shows the decrease in power of bands 20-40Hz preceding the movement, and then the "post-movement rebound" (increase in power) after the movement is completed, which has also been reported in previous studies (Jurkiewicz, et al. 2006). We also see an increase of the low frequency activity in the period that precedes the movement, which some researchers have associated in the past with a motor readiness field (Salmelin, et al. 1995). Finally, the picture shows a 30% increase in the power of frequencies

from 70-90Hz, similar to what has been reported before for local field potential recordings (Heldman, et al. 2006).

The final step in this analysis was to verify if the frequency modulation seen above is tuned to particular targets. Figure 11 reveals that the patterns seen before are still present in a target by target basis for both overt and imagined conditions. However, it is noticeable that the amount of modulation for the overt movement is considerable stronger than the modulation of the same bands in imagined movement. Still, for both conditions it is possible to note differences in the modulation based on target position, and this difference will be used as the basis for decoding target position from the data.

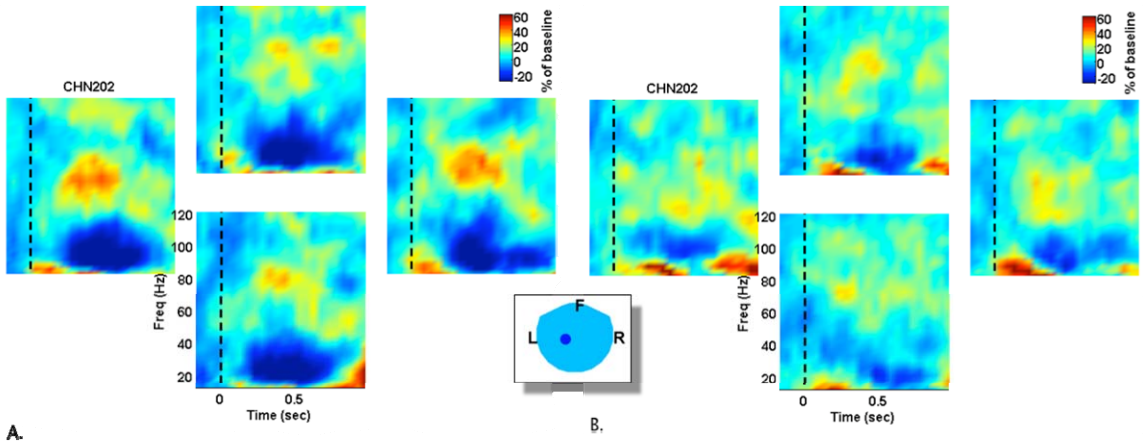

Figure 11: Frequency modulation over time for each specific target. Position of the spectrograms corresponds to their associated targets. The first four plots (A) correspond to overt movement, and the last 4 (B) show data from the imagined condition. Data averaged over all repetitions of a given target (162 – subject S3), aligned on visual cue onset.

3.3 DECODING

After scoring the features with p-values as described in the Methods section, both OLE and Bayesian estimators were used to predict target direction. Only the 100 features with the smallest p-values (all smaller than 0.05) were used for decoding, because that not only sped up the decoding time, but it helped to remove unstable features (i.e. features that did not show similar behavior for the majority of repetitions). The same feature space was used for decoding with OLE and Bayesian algorithms.

Figure 12 shows the results of single trial decoding for both overt and imagined movements using Bayesian and OLE for decoding. Decoding results varied tremendously across subjects, and it is clear that the features do not tend to favor all targets equally. Still, both decoding methods achieved accuracies well above chance level for the majority of targets and subjects. Accuracy for overt movement was higher than in imagined as expected in both decoders, peaking 69.5% for subject S3 in OLE and 68% with Bayesian. Accuracy in imagined movements peaked at 50% accuracy for three of the subjects using both methods of decoding.

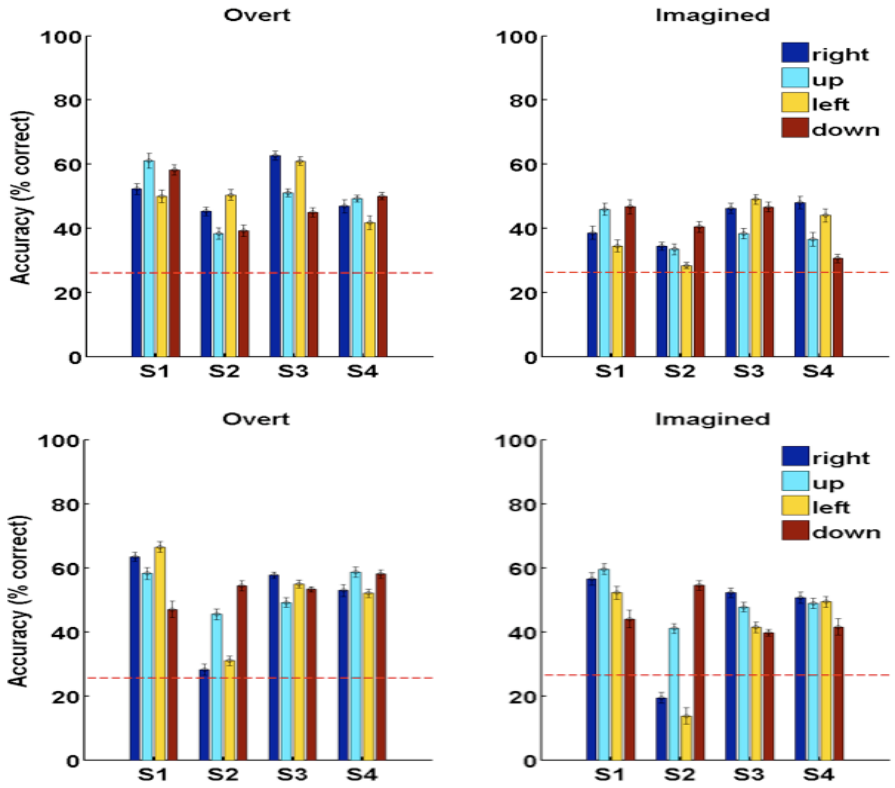

Figure 12: Single trial decoding results for OLE and Bayesian decoders (left and right, respectively) for overt (top) and imagined (bottom) conditions. Horizontal dashed line represents chance level. Results obtained with leave-one-out method using 80% of the total number of repetitions for each subject (overt – imagined, S1: 72 – 82, S2: 122 – 142, S3: 129 – 107, S4: 108 – 100). Error bars show the standard error from running the leave-one-out method 20 times, selecting the repetitions at random from the total pool of repetitions of each subject.

The next step was to plot where these 100 best features used in the decoding were situated in the MEG helmet. Figure 13 shows the spatial relationship of these features used for the subject with the best accuracy results (S3).

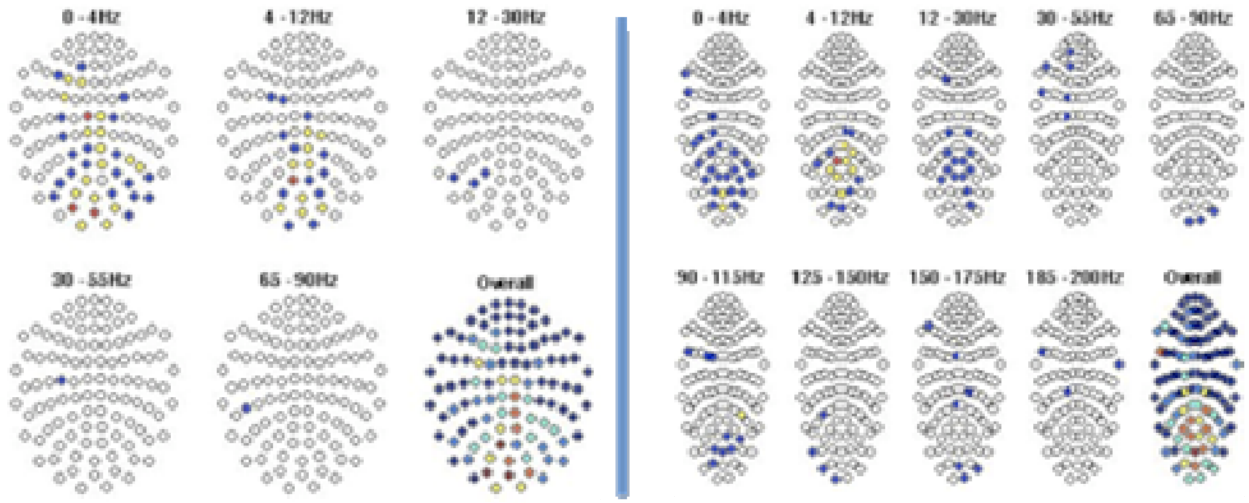

Figure 13: Spatial distribution of the 100 best features used for decoding (subject S3). Plots on the left are for overt condition and the right for imagined. Each helmet has 102 sensor positions and their colors indicate how many channels were used as features for that particular frequency band: white – 0, blue – 1, yellow – 2, red – 3. Overall plots are a summation of all features in all bands used. Hotter colors represent more features for that sensor.

Although this subject did not have features above 90Hz among the best ones for the overt condition, it is clear that the majority of his features are around the sensors covering regions involved in the movement (visual, parietal, motor). The imagined condition showed features in very high frequencies for areas involved in the movement, but also in sensors that are not directly related to the task. Still, the majority of its features surrounded visual and parietal regions, as shown in the overall plot.

One of the drawbacks of choosing the best features solely by their p-values is ignoring the spatial organization of the sensors in the helmet. Although the majority of the features used in the decoding were located in the regions directly related to the movement, it was interesting to check if the decoding results would improve if the features used were further restricted to the sensorimotor region only. This region was arbitrarily chosen as depicted in Figure 14, which also

shows the relationship of all significant low-frequency features across the sensorimotor areas between overt and imagined conditions. This figure summarizes the idea that the majority of the features seen in the sensorimotor region during overt movement are also present in imagined tasks.

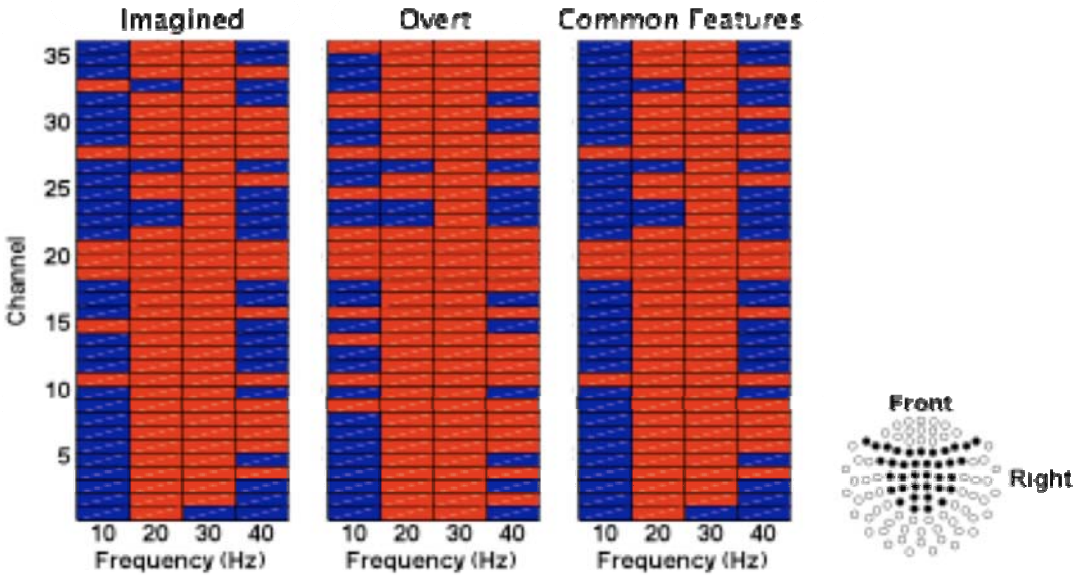

Figure 14: Low-frequency features (0-40Hz) and their significance for all channels in the sensorimotor band. Red means that their p-value was below 0.05. Tables show the features present in imagined and overt movements for subject S3. The right-most table shows the intersection of the first two. Also shown in the picture the layout of the sensors chosen as part of the sensorimotor area.

Decoding results using the best features restricted to the sensors on top of sensorimotor area are shown in Table 1. For all subjects, restricting the features decreased the average decoding accuracy. In other words, there is important information relative to target position in sensors other than the ones selected as part of the sensorimotor area. Still, it is not always true that the accuracy of decoding will be proportional to the number of features used: when all significant features were used for decoding (instead of just the 100 best ones), the accuracy went

down, meaning that some features were either too noisy or inversely contributed to the accuracy of the decoding.

Table 1: Decoding accuracies (%) averaged across targets for overt and imagined conditions. OLE decoder was used to compare the accuracies of movement decoding using all the best features against using only the ones covering the sensorimotor cortex.

Subjects	Overt		Imagined	
	Best	Sensorimotor	Best	Sensorimotor
S1	55 (±2.11)	43.54 (±1.91)	43.07 (±1.82)	40.52 (±1.78)
S2	39.16 (±1.42)	34.96 (±1.65)	39.50 (±1.39)	35.46 (±1.53)
S3	54.70 (±1.32)	49.03 (±1.43)	41.85 (±1.50)	40.27 (±1.93)
S4	44.50 (±1.75)	42.89 (±1.48)	41.01 (±1.73)	34.67 (±1.61)

Finally, decoding using averaged data was performed. These results are displayed in Figure 15, which plots decoding accuracy as a function of number of repetitions averaged for decoding. The signal-to-noise ratio (SNR) in MEG is relatively low, so averaging the repetitions promotes increase in SNR and subsequently improves accuracy. Therefore, the decoding results for both imagined and overt conditions increased with data-averaging as expected. However, decoding overt movement seemed to gain the most with this approach because after 8 repetitions it had close to 100% accuracy for both OLE and Bayesian decoders. With 10 averaged repetitions the imagined condition still had decoding accuracies between 70 – 90% for both OLE and Bayesian decoders.

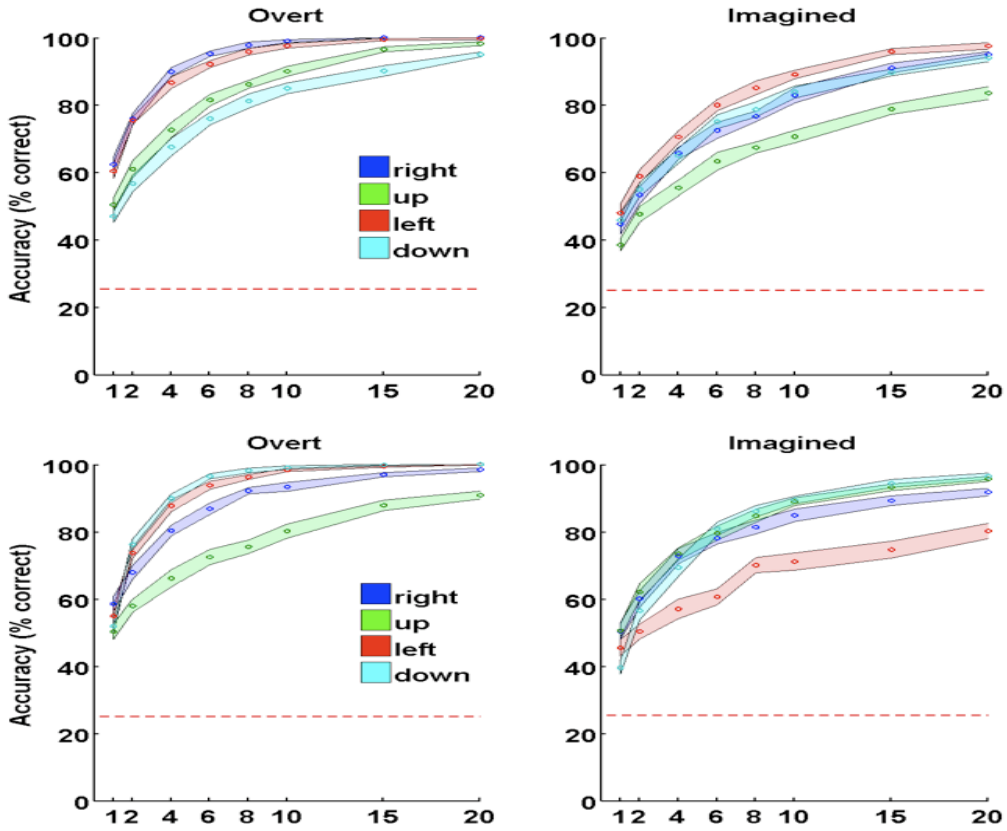

Figure 15: Decoding results for averaged data of subject S3. Horizontal axis shows how many repetitions were averaged before testing to obtain the accuracy in vertical axis. Training was done in 129 and 107 (overt and imagined, respectively) repetitions. Shaded fills around traces represent 95% confidence interval after running the leave-one-out method 20 times.

4.0 DISCUSSION

This study characterized the MEG activity during overt and imagined wrist tasks. The temporal evolution of the MEG signal amplitude over the course of a center-out movement was consistent across all four subjects. In the frequency domain, the decrease in activity of low frequency bands preceding movement and the rebound when the movement is finished were also consistent within the subject population. Also consistent was the increase in power of 0-10Hz. On the other hand, the increase in power of higher bands was less salient and the degree of power increase varied among the subjects.

Decoding of target choice (i.e. movement direction) based on MEG data has also been accomplished with accuracy above chance level for single-trial decoding. The method for selecting the features used for decoding had a big impact in the final results, but using the 100 best features as shown before gave the highest accuracy of decoding. Although restricting features used for decoding to those from sensors located on top of the sensorimotor cortex did not improve the decoding accuracy, it is important to note that the definition of a sensorimotor area in the sensor space is very coarse and therefore very subjective. In order to truly select features coming from the sensorimotor region, a source localization technique would need to be employed prior to using the data for decoding.

Both OLE and Bayesian decoders showed similar results for target prediction. Bayesian results can potentially be higher if different models of the probability distributions are used to

better fit the data, and if the correlation between features is taken into account when combining the probabilities obtained for individual features. In terms of computational cost, OLE was noticeable faster as the number of features increased, which will be an important factor later for real-time decoding if the number of features needed is much bigger than 100.

Finally, the high accuracy results obtained by decoding on averaged data suggest that the information about target position is embedded in the data, but the MEG signal is too noisy to be used for single-trial decoding and still obtain such high accuracy results. Still, new approaches for data analysis and feature selection (see Future Work) may increase the accuracy of single-trial decoding using the same dataset as before. It is true that achieving this goal is crucial for using MEG as a real-time BCI research tool, but it has been shown that the cortical activity is plastic and it adapts to the decoding algorithm and the degree of signal modulation increased with real-time closed-loop brain-controlled cursor movement training (Taylor, Tillery and Schwartz 2002). Therefore, it is expected that during real-time MEG-controlled cursor movement, the plasticity of the subject's brain signals may also play an important role in increasing the signal-to-noise ratio of the MEG recordings, this way improving the decoding accuracy on itself.

5.0 FUTURE GOALS

This work has been successful in proving the feasibility of using MEG to conduct BCI research, as well as studying cortical representation of movement. Still, several areas can be identified that could potentially further improve this work, either by improving the accuracy of the results or by offering different insights in the cortical processes studied here.

5.1 TIME-POINT DECODING

The target decoding presented here is essentially a classification problem for four different categories (up, down, left, and right) based on multiple features from MEG signals (specific frequency bands from specific MEG sensors). For a real-time BCI system, cursor position needs to be updated in a very fast rate (> 10 to 20 times per second), and it is desirable for the subject to be able to move the cursor on the computer screen in arbitrary directions instead of the four specific discrete categories. Therefore, it will be interesting to test whether the position and/or the velocity of the cursor can be decoded continuously in time instead of using the average activation over a certain period of time. Furthermore, the current study used frequency band power to decode target direction. However, previous studies in MEG and ECoG have suggested that rich movement-related modulation also exist in the very low frequency band (<3 Hz) and in

time domain signals. Thus, it is worth trying to decode target direction using the MEG signals in the time domain, instead of converting it to the frequency domain in the beginning as done here.

In theory, this could be accomplished by repeating the same decoding schemes used here using a sliding window (e.g. 200~300 ms) with a small time step (e.g. 50 ms) to predict instantaneous cursor movement velocity vector. The movement to target is essentially the integration of the cursor velocity over time.

5.2 DELAY ANALYSIS: PLANNING VS. MOVEMENT

There is a big debate about whether the information decoded here comes from the intention of movement (motor commands) or if sensory processes (e.g. visual feedback of the cursor position) provide the main source of information used in the decoding analysis.

In order to try to answer this question, two subjects were scanned using a paradigm that included a variable delay period before the subjects were asked to move. More specifically, after the period of holding the cursor in the center was over, one of the peripheral targets would appear but the center target did not disappear. The subject was instructed to only move to the target when the center target disappeared (go-cue), which happened within 0.5-1.5s after the presentation of the peripheral targets. The same change was applied to the imagined sessions, but in that case the subjects were asked to only start imagining the wrist movement when the center target disappeared.

The goal of implementing this modification was to try to decode the target choice based only in the planning period (excluding the movement time), and compare that with the results obtained when decoding using data from both planning and movement time. Also, it would be

interesting to analyze the frequency modulation and temporal patterns in the MEG sensors while the subject is planning the movement.

The initial results from this analysis show that similar decoding accuracy seen using the data of planning and movement can be obtained from just using the planning data (from target onset to movement onset), for this specific wrist task. Decoding target position using just the movement data (from movement onset to movement offset) did not show a decoding accuracy comparable to previous results.

5.3 DIFFERENT APPROACHES FOR DATA ANALYSIS

Different techniques in the data analysis process can also be tried in order to obtain better results. Firstly, it is known from the data that some MEG sensors show very high correlation in temporal domain. It is also known that the MEG signal-to-noise ratio is low compared to other recordings techniques, especially for higher frequency bands (> 40 Hz). Thus, it may be beneficial to combine these correlated MEG sensors in a way to reduce noise and decrease the dimensionality of the data. The first method one may try is to combine MEG signals (by using Principal Component Analysis, Pitagorean sum, or any other method) recorded from the two gradiometers that are positioned in the same location in the helmet. However, the highest correlation values in the data (in the temporal domain) do not necessarily come from gradiometers at the same sensor location, so ideally this method should be run for any pair of highly correlated channels.

Another approach that may improve the decoding results would involve choosing a better method to select the frequency bands used for decoding. This work used frequency bands well-known in the literature to be involved with sensorimotor processes, such as 1-3Hz, 4-12Hz and

10-30Hz. However, there is little work relating the function of higher frequencies to this task. The approach used in this experiment was to take small incremental steps to cover all ranges up to 200Hz (65-75Hz, 75-85Hz, etc). Alternatively, one can use a sliding window of a certain width (e.g. 10 Hz) and slide it across 0 to 200 Hz with a small step size (e.g. 2~3 Hz) to find the frequency bands that contain significant information about movement direction. Then, those frequency bands can be used to further improve decoding accuracy.

Finally, the work done in the frequency domain used as a measure the percent change of power with respect to a baseline. Here, baseline was defined as the time the subject held the cursor in the center. Although this can be considered an unbiased estimate of the baseline (i.e. there is no preference for any of the targets), it may be the case that using other periods for baseline would result in more meaningful percent changes for decoding. Other options one may want to try in the future are the baseline acquired in the beginning of recording sessions (the subject is resting staring at the center of the screen), an average of all hold-center baselines, or the average of the activity during the planning and movement for all targets.

5.4 STATISTICAL METHODS

Several assumptions are made when conducting the analysis described here. In particular, some of the assumptions that could be improved upon are related to the Bayesian decoding. Each feature used to decode target choice had its own prediction for a given repetition, and all these predictions were multiplied to obtain a final prediction for the repetition. Such method assumes that the features are independent of each other, which is not completely true. Because some of the channels are located in the same sensor, some of their signals are very likely to be correlated.

In fact, many channels showed high correlation in time domain even when they did not share a sensor. Ideally, one would make the features as independent as possible before using them in this Bayesian decoding algorithm.

Another improvement that could be made to the Bayesian decoding is the way in which the probabilities of a target for a given feature are obtained. One could try to model these probabilities with different known distributions, and maybe this way even account for the correlation between channels. Also related to decoding, having a better way to select the best features (instead of the ANOVA, which assumes the normality of the data) may help increase accuracy. Feature selection is a very active topic in machine learning, which means that there are innumerous options from which one could choose, but non-parametric methods such as Kruskal-Wallis or looking at covariances to pick more stable features could be a good start.

Finally, one could look at the correlation between different channels to do the decoding instead of the signals themselves (Langheim, Leuthold and Georgopoulos 2006). It would also be interesting to look at Granger causality in this situation.

5.5 REAL TIME MEG

One of the future goals of this work is to have the subject control the cursor with his or her brain activity using the MEG signals in real-time. It is expected that the brain will adapt to the classification method used here, and therefore the signal-to-noise ratio will go up. A real-time MEG-based BCI system can be used for user training and pre-surgical screening of optimal implantation sites for future BCI devices based on implanted microelectrodes.

Considerable work has been done in the course of this project to capture the MEG signals in real time. At the present, we can interact with the MEG system and capture the signals in real time with a maximum lag of 32ms. This was measured by using a function generator to send a sine wave to the MEG acquisition system through its sensors and also its A/D converter. An auxiliary PC read the sine wave recorded by the MEG system using UDP and sent a pulse to the MEG system with polarity based on the sign of the sine wave. This pulse signaled to the MEG system the time when the PC identified the sine wave. Finally, the delay was measured by only using the data recorded in the MEG system, calculating the difference between the sine wave (e.g. the actual data) and the pulse (when the PC "saw" the data). Figure 16 describes the test that was used to measure the inherent delay for streaming the MEG data in real-time.

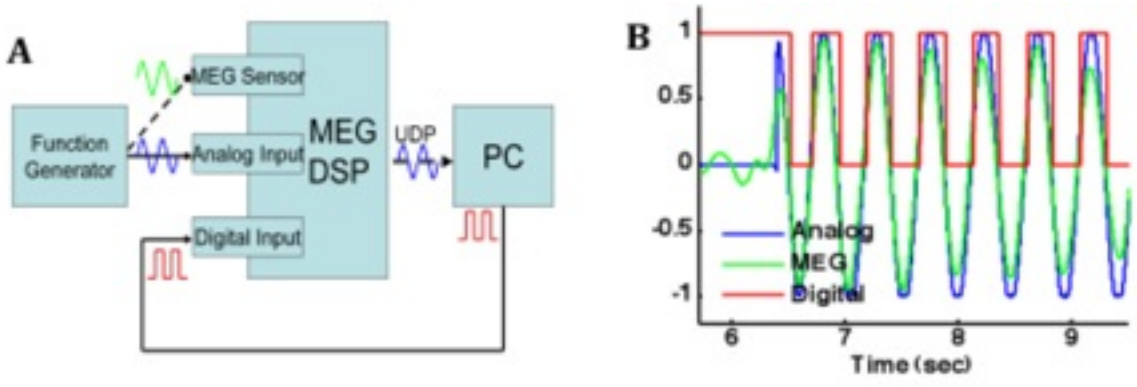

Figure 16: Experiment to test real-time MEG delay. **A.** The computer recording MEG signals received a sine wave as an analog input and also as a measurement by its sensors. It also received a pulse generated by the computer that received the data packets with the MEG data. **B.** Plotting the two signals sent on the network by the MEG machine against the pulse generated by the recording computer.

The next step towards a real-time MEG-BCI system and have the subject control the cursor with brain activity is to develop a software module that interfaces with our current BCI2000 platform software, which should be ready shortly.

5.6 SOURCE LOCALIZATION

While the current analysis has all been done in the sensor space, it is evident that the spatial resolution of such method is low because each MEG sensor records brain activity averaged over a large area. Also, the position of the sensor with respect to the cortex highly depends on the head shape, as well as its position with respect to the MEG helmet. One of the goals of this project to eventually map the MEG activity from the MEG sensor space onto the cortex and therefore to better characterize the anatomical location of the source of MEG signals being analyzed in this study.

Another challenge to be taken in future endeavors is to check if decoding the target direction using signals that have been previously localized to certain parts of the brain will increase accuracy. If that is true, then a second difficult task would be to identify an optimal source localization algorithm that would perform its operations within a short time frame, which is necessary in order to make these signals feasible for real time control.

BIBLIOGRAPHY

Amorim, M A, W Lang, G Lindinger, D Mayer, L Deecke, and A Berthoz. "Modulation of spatial orientation processing by mental imagery instructions: a MEG study of representational momentum." *J Cogn Neurosci* 12, no. 4 (2000): 569-582.

Cheyne, D, S Bells, P Ferrari, W Gaetz, and A Bostan. "Self-paced movements induce high-frequency gamma oscillations in primary motor cortex." *NeuroImage* 42, no. 1 (Aug 2008): 332-342.

Crone, N, D Boatman, B Gordon, and L Hao. "Induced electrocorticographic gamma activity during auditory perception." *Clinical Neurophysiology*, Jan 2001.

Diekmann, V Erne S, and W Becker. "Magnetoencephalography." Aug 1999: 30.

Druschky, K, et al. "Somatosensory evoked magnetic fields following passive movement compared with tactile stimulation of the index finger." *Exp Brain Res* 148, no. 2 (2003): 186-195.

Fabiani, Georg E, Dennis J McFarland, Jonathan R Wolpaw, and Gert Pfurtscheller. "Conversion of EEG activity into cursor movement by a brain-computer interface (BCI)." *IEEE transactions on neural systems and rehabilitation engineering : a publication of the IEEE Engineering in Medicine and Biology Society* 12, no. 3 (Sep 2004): 331-8.

Georgopoulos, A P, A B Schwartz, and R E Kettner. "Neuronal population coding of movement direction." *Science* 233, no. 4771 (1986): 1416-9.

Georgopoulos, AP, et al. "Synchronous neural interactions assessed by magnetoencephalography: a functional biomarker for brain disorders." *J Neural Eng* 4, no. 4 (2007): 349-355.

Georgopoulos, Apostolos P, Frederick J P Langheim, Arthur C Leuthold, and Alexander N Merkle. "Magnetoencephalographic signals predict movement trajectory in space." *Exp Brain Res* 167, no. 1 (2005): 132-135.

Hämäläinen, M, R Hari, R Ilmoniemi, and J Knuutila. "Magnetoencephalography—theory, instrumentation, and applications to noninvasive studies of the …." *Reviews of Modern Physics*, Jan 1993.

Hari, R, and N Forss. "Magnetoencephalography in the study of human somatosensory cortical processing." *Philos Trans R Soc Lond B Biol Sci* 354, no. 1387 (1999): 1145-54.

Heldman, Dustin A, Wei Wang, Sherwin S Chan, and Daniel W Moran. "Local field potential spectral tuning in motor cortex during reaching." *IEEE transactions on neural systems and rehabilitation engineering : a publication of the IEEE Engineering in Medicine and Biology Society* 14, no. 2 (Jun 2006): 180-3.

Jurkiewicz, Michael T, William C Gaetz, Andreea C Bostan, and Douglas Cheyne. "Post-movement beta rebound is generated in motor cortex: evidence from neuromagnetic recordings." *NeuroImage* 32, no. 3 (Sep 2006): 1281-9.

Kaiser, J, B Ripper, N Birbaumer, and W Lutzenberger. "Dynamics of gamma-band activity in human magnetoencephalogram during auditory pattern working memory." *NeuroImage*, Jan 2003.

Kakei, S, D S Hoffman, and P L Strick. "Muscle and movement representations in the primary motor cortex." *Science (New York, NY)* 285, no. 5436 (Sep 1999): 2136-9.

Kim, June Sic, and Chun Kee Chung. "Language lateralization using MEG beta frequency desynchronization during auditory oddball stimulation with one-syllable words." *NeuroImage* 42, no. 4 (Oct 2008): 1499-507.

Langheim, Frederick J P, Arthur C Leuthold, and Apostolos P Georgopoulos. "Synchronous dynamic brain networks revealed by magnetoencephalography." *PNAS* 103, no. January (Nov 2006): 5.

Leuthardt, Eric C, Gerwin Schalk, Jonathan R Wolpaw, Jeffrey G Ojemann, and Daniel W Moran. "A brain-computer interface using electrocorticographic signals in humans." *J Neural Eng* 1, no. 2 (2004): 63-71.

McFarland, D, A Lefkowicz, and J Wolpaw. "DESIGN AND OPERATION OF AN EEG-BASED BRAIN-COMPUTER INTERFACE WITH DIGITALSIGNAL PROCESSING …." *Behavior research methods*, Jan 1997.

Mellinger, Jurgen, et al. "An MEG-based brain-computer interface (BCI)." *Neuroimage* 36, no. 3 (2007): 581-593.

Moran, D W, and A B Schwartz. "Motor cortical activity during drawing movements: population representation during spiral tracing." *Journal of neurophysiology* 82, no. 5 (Nov 1999): 2693-704.

Neuromag, Elekta. "MaxFilter User's Guide." no. October (Nov 2006): 64.

—. "System Description - Magnetoencephalographic and Electroencephalographic System." Mar 17, 2006. 32.

Salinas, E, and L F Abbott. "Vector reconstruction from firing rates." *J Comput Neurosci* 1, no. 1-2 (1994): 89-107.

Salmelin, R, N Forss, J Knuutila, and R Hari. "Bilateral activation of the human somatomotor cortex by distal hand movements." *Electroencephalogr Clin Neurophysiol* 95, no. 6 (1995): 444-452.

Schalk, G, D McFarland, and T Hinterberger. "BCI 2000: A General-Purpose Brain-Computer Interface(BCI) System." *IEEE Transactions on Biomedical Engineering*, Jan 2004.

Schwartz, Andrew B, X Tracy Cui, Douglas J Weber, and Daniel W Moran. "Brain-controlled interfaces: movement restoration with neural prosthetics." *Neuron* 52, no. 1 (2006): 205-20.

Taulu, S, J Simola, and M Kajola. "Applications of the Signal Space Separation Method." … *Acoustics*, Jan 2005.

Taylor, D, S Tillery, and A Schwartz. "Direct Cortical Control of 3D Neuroprosthetic Devices." *Science*, Jan 2002.

Waldert, S, H Preissl, E Demandt, and C Braun. "Hand Movement Direction Decoded from MEG and EEG." *Journal of Neuroscience*, Jan 2008.

Wang, Wei, Sherwin S Chan, Dustin A Heldman, and Daniel W Moran. "Motor cortical representation of position and velocity during reaching." *Journal of neurophysiology* 97, no. 6 (Jun 2007): 4258-70.